Generic solving of physiologically-based kinetic models in support of next generation risk assessment due to chemicals

Sandrine CHARLES[1]*, Ophelia GESTIN[1,2,3], Jérémie BRUSET[1], Dominique LAMONICA[1], Virgile BAUDROT[4], Arnaud CHAUMOT[2], Olivier GEFFARD[2] and Christelle LOPES[1]

[1]University of Lyon, University Lyon 1, UMR CNRS 5558, Villeurbanne, France

[2]INRAE, Riverly, Ecotoxicology, Lyon, France

[3]University of La Rochelle, UMRi 7266, La Rochelle, France

[4]Qonfluens, Rdpt Benjamin Franklin, Montpellier, France

April 28, 2022

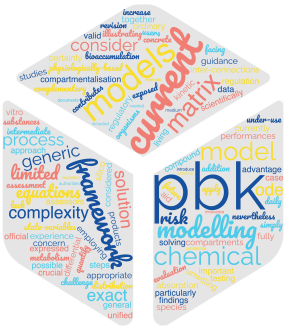

*Corresponding author: sandrine.charles@univ-lyon1.fr

Abstract

Increase the confidence in using *in vitro* and *in silico* data to aid the chemical risk assessment process is one, if not the most, important challenge currently facing regulatory authorities. A particularly crucial concern is to fully take advantage of scientifically valid physiologically-based kinetic (PBK) models. Nevertheless, risk assessors remain still unwilling in employing PBK models within their daily work. Indeed, PBK models are not often included in current official guidance documents. In addition, most users have limited a limited experience in using modelling in general. So, the complexity of PBK models, together with a lack to evaluation methods of their performances, certainly contributes to their under-use.

This paper proposes an innovative and unified modelling framework, in both the writing of PBK equations as matrix ordinary differential equations (ODE), and in its exact solving simply expressed with matrix products. This generic PBK solution allows to consider as many as state-variables as needed to quantify chemical absorption, distribution, metabolism and excretion processes within living organisms when exposed to chemical substances. This generic PBK model makes possible any compartmentalisation of the model to be considered, as well as all appropriate inter-connections between compartments and with the external medium.

We first introduce our PBK modelling framework, with all intermediate steps from the matrix ODE until the exact solution. Then we apply this framework to bioaccumulation testing, before illustrating its concrete use through complementary case studies in terms of species, compound and model complexity. Upon our findings, we finally propose to consider this approach to eventually be part of a future revision of the current regulation.

Keywords

Pharmacokinetics, Toxicokinetics, General unified modelling framework, Bioaccumulation, Chemical exposure.

---

1 Introduction

Physiologically-Based Kinetic (PBK) models encompass both pharmaco- (PBPK) and toxicokinetic (PBTK) models depending on the context referring either to toxicity risk assessment [14, 19] or therapeutic drug development [35]. All PBK models are compartment models employing ordinary differential equations (ODE) to quantify chemical absorption, distribution, metabolism (*i.e.*,biotransformation) and excretion (ADME) processes within living organisms when exposed to chemical substances [33]. One fundamental aspect of PBK model complexity is the degree of compartmentalization (*i.e.*, differentiation of an organism into various tissues or organs) [3]. Moreover, some PBK models may have purely predictive uses, for example for human health assessments where experiments are very limited, even impossible [20]. Nevertheless, recent advances in the development of Bayesian inference tools make today possible to deal with complex models [12, 28, 30]. Also, as part of New Approach Methodologies (NAM), PBK models as well as *in vitro-in vivo* extrapolation (IVIVE) approaches can be combined with bioactivity data for prioritizing thousands of "data poor" chemicals in human health risk assessment [3, 6].

Relying *a priori* on the anatomical and physiological structure of the body, PBK model compartments usually correspond to target organs or tissues, possibly all interconnected and related to the external exposure medium. However, a lot of PBK models relate organs or tissues to corresponding to only blood or lymph, on or two organ or tissue being related to the external medium [36, 34]. PBK models are thus written as coupled ODE whose parameters corresponding to fluxes between compartments, for which information is partly available in scientific publications. Given the immense computational capacities available today, and the general tendency to make models ever more complex to include as many physiological processes as possible, could give the impression that the most complex models will be the most efficient. Nevertheless, with an increasing number of parameters to calibrate, such complex models may usually be avoided, with a balanced compromised to find between complexity and simplicity. As a matter of fact, current regulatory documents for assessing the bioaccumulation of chemicals in organisms usually only require one-compartment models [22, 24, 25, 8]. However, it may be necessary to consider not only the total concentration within the organisms, but rather internal concentrations within target organs [32].

Multi-compartment models reveal sometimes absolutely necessary, for example in finely deciphering the internal contamination routes of specific chemical compounds that cause damages to only target organs [7, 1, 13]. Additionally, PBK models can be of crucial importance to predict organ-level concentration–time profiles in situation where animal testing is now prohibited, using PBK model information from one chemical substance to inform the development or evaluation of a PBK model for a similar chemical substance [31]. For such purpose, but also to enlarge the use of PBK models, there is today a clear need for user-friendly tools facilitating the implementation of any PBK models, whatever the required number of compartments to consider, whatever the number of connections to account for between compartments in pairs of between compartment and the external medium, and whatever the species-compound combination of interest. This seems the only way to gradually achieve greater acceptability of these apparently complex PBK models in a regulatory context [23, 3].

Capitalizing on recent publications on TK models [25, 8], we present in this paper a very innovative exact solution of a fully generic PBK model written as a set of ODE. Our modelling framework makes possible to account for a infinite number of compartments, with all possible connections between pairs of compartments and between compartments and the exposure medium, independently of the species and of the chemical substance to deal with. Indeed, we found a particularly condensed way to write a linear ODE system as typically are PBK models, thus allowing us to fully and exactly solve the ODE system to write a generic exact solution. This exact solution reveals particularly interesting when estimating a large number of parameters related to many state variables and for which experimental data may be sparse, with few replicates and a high variability. In the following sections, we first detail our generic modelling framework, together with notations of parameters and variables, providing the generic solution a the end of section 2. In section 3, the generic modelling framework is applied to the particular context of bioaccumulation of chemical substances within organisms. We detail how to write the ODE system for both accumulation and depuration phases of standard bioaccumulation tests, and then how to get the final generic solution to simulate internal concentrations over time from parameter estimates. Lastly, section 4 presents three different situations where simulations revealed useful to predict what happens

within organs and/or tissues according to the species under consideration, and to the chemical substance to which it is exposed. These case-studies were chosen from the literature to be both diverse and complementary in terms of questioning which a PBK model can help to investigate.

2 Generic modelling framework

Biologists will often have the tendency to expect an exhaustive description of phenomenon in which they are interested. In the same way, mathematicians will want to use the most sophisticated methods they know. However, all models are inherently wrong, only some of them will prove useful [5]. As a consequence, the modeller should position between these two extremes to be efficient. This point of view is known as the *parsimony principle* by which the simplest model that adequately explains the data should be used; it was proposed in the 14th century by William of Ockam, an English Franciscan friar, scholastic philosopher, and theologian [16]. In its general form, the parsimony principle, also referred to as Occam's Razor, states that the simplest of competing explanations is the most likely to be correct. In the context of model fitting, the simplest model providing a good fit will be preferred over a more complex one. The compromise is thus between good fit and simplicity.

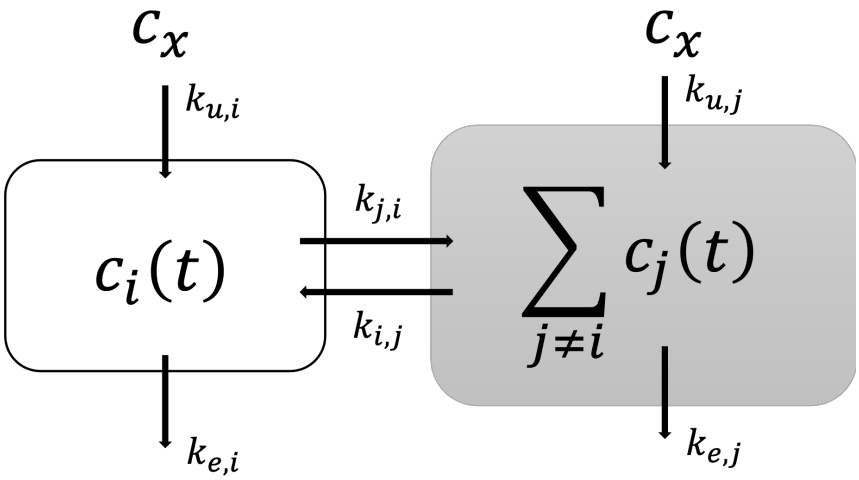

Figure 1: Generic scheme of a multi-compartment toxicokinetic model connecting n compartments two-by-two and each of them to the external medium at exposure concentration c_x. Refer to Table 1 for names, meaning and units of variables and parameters.

In this spirit, the most generic PBK models will rely on simplifying hypotheses, to both decipher enough internal mechanisms under chemical exposure, and remain mathematically reasonable so as to be easily manipulated. Below is a non-prioritized short list of the most current hypotheses: (i) the exposure concentration is assumed constant over time; (ii) there can be any number of compartments in direct relation with the number of tissues and organs to consider; (iii) all compartments can potentially be connected two-by-two to all others; (iv) all compartments can potentially be connected to the external medium; (v) the exposure concentration can potentially enter within each compartment.

From these hypotheses, Figure 1 gives the general schematic representation of exchanges between the external medium and compartments, as well as between compartments themselves. Table 1 gathers all variables and parameters involved in the generic writing of the PBK model, and used in Figure 1.

Names	Meaning	Unit
t	time	$[t]$
n	total number of compartments	#
i, j	Compartment numbers	$i, j \in [1; n]$
c_x	exposure concentration in the external medium	mass per volume
$c_i(t)$	internal concentration in compartment i at time t	mass per weight
$k_{u,i}$	uptake rate from the external medium to compartment i	$[t]^{-1}$
$k_{e,i}$	elimination rate from compartment i to the external medium	$[t]^{-1}$
$k_{i,j}$	input rate from compartment j to compartment i	$[t]^{-1}$
$k_{j,i}$	output rate from compartment i to compartment j	$[t]^{-1}$

Table 1: Variable and parameter names, meaning and unit as used within the generic PBK model all a long this paper. Symbol # means dimensionless; $[t]$ stands for time unit.

2.1 Mathematical equations of the PBK model

From Figure 1, we can derive the full system of ordinary differential equation (ODE) describing the dynamics of the multi-compartment model when organisms are exposed to an external concentration c_x:

$$\frac{dc_i(t)}{dt} = k_{u,i}c_x - k_{e,i}c_i(t) + \sum_{j \neq i} k_{i,j}C_j(t) - \left(\sum_{j \neq i} k_{j,i}\right) c_i(t) \quad \forall i, j \in [1; n] \tag{1}$$

Names, meaning and units of variables and parameters are provided in Table 1.

This full system of ODE for n compartments all related by pairs (equation 1) can equivalently be written in a matrix way as follows:

$$\frac{d\mathbf{C}(t)}{dt} = \mathbf{U}\, c_x + \mathbf{E}\, \mathbf{C}(t) \tag{2}$$

where vector $\mathbf{C}(t)$ gathers all internal concentrations in compartments i at time t, $i \in [1; n]$:

$$\mathbf{C}(t) = \begin{pmatrix} c_1(t) & c_2(t) & \dots & c_n(t) \end{pmatrix}^T \tag{3}$$

Vector $\mathbf{U}$ contains all uptake rates from the external medium at exposure concentration c_x:

$$\mathbf{U} = \begin{pmatrix} k_{u,1} & k_{u,2} & \dots & k_{u,n} \end{pmatrix}^T \tag{4}$$

Matrix $\mathbf{E}$ gathers both input and output rates between compartments two-by-two, together with the elimination rates from each compartment i, $i \in [1; n]$:

$$\mathbf{E} = [e_{ij}]_{i,j \in [1;n]} \quad \text{with} \quad \begin{cases} e_{ii} = -k_{e,i} - \sum\limits_{j \neq i} k_{j,i} \\ e_{ij} = k_{i,j} \end{cases} \tag{5}$$

Equation (2) is a matrix ODE system, which is linear with a second member. Its solving can be performed in two steps as detailed below.

2.2 Generic solving the PBK model

The first step is to solve the matrix system (2) without its second member. Then, using the method of the variation of constant, the second will consist in finding the final general solution.

2.2.1 Solving the ODE system without the second member

Removing the second member from the matrix ODE system (2) leads to the following system to solve:

$$\frac{d\mathbf{C_{wosm}}(t)}{dt} = \mathbf{E}\,\mathbf{C_{wosm}}(t) \tag{6}$$

with $\mathbf{C_{wosm}}(t)$ the desired solution of equation (6). Using matrix exponential immediately provides the solution:

$$\mathbf{C_{wosm}}(t) = e^{t\mathbf{E}}\mathbf{\Omega_1} \tag{7}$$

with $\mathbf{\Omega_1}$ a vector integration constant ($\in \mathbb{R}^n$), and the following definition for the matrix exponential:

$$e^{t\mathbf{E}} = \sum_{j=0}^{\infty} \frac{1}{j!} (t\mathbf{E})^j \tag{8}$$

2.2.2 Getting the generic solution of the ODE system

For the second step in solving of matrix ODE system including the second member, we used the method of the variation of the constant, starting from the assumption that the general final solution can be written as follows:

$$\mathbf{C_{wsm}}(t) = e^{t\mathbf{E}}\mathbf{\Omega_1}(t) \tag{9}$$

with a vector function $\mathbf{\Omega_1}(t)$ to determine.

Given that the exposure concentration is assumed constant (equal to c_x)in this paper, deriving equation (9) and replacing terms in equation (2) leads to the following result:

$$\frac{d\mathbf{\Omega_1}(t)}{dt} = e^{-t\mathbf{E}}\mathbf{U}c_x \Leftrightarrow \mathbf{\Omega_1}(t) = \left(\int_0^t e^{-\tau\mathbf{E}} d\tau\right)\mathbf{U}c_x + \Omega_2 \tag{10}$$

The final generic solution of equation (2) will thus write as:

$$\mathbf{C_{wsm}}(t) = \left(\int_0^t e^{(t-\tau)\mathbf{E}} d\tau\right)\mathbf{U}c_x + e^{t\mathbf{E}}\mathbf{\Omega_2} \tag{11}$$

with $\mathbf{\Omega_2} \in \mathbb{R}^n$ a constant to determine.

From an initial condition $\mathbf{C_{wsm}}(t) = \mathbf{C_0}$, we finally get $\mathbf{\Omega_2} = \mathbf{C_0}$, what leads to this final particular solution of equation (2):

$$\mathbf{C_{wsm}}(t) = \left(\int_0^t e^{(t-\tau)\mathbf{E}} d\tau\right)\mathbf{U}c_x + e^{t\mathbf{E}}\mathbf{C_0} \tag{12}$$

It remains now to calculate the matrix integral to achieve the very final solution of the matrix ODE system (2).

2.2.3 Final expression solution of the PBK solution

As detailed in the Supplementary Information (SI), and using the definition of a matrix exponential from equation (8), the matrix integral in equation (12) can be calculated with the following expression:

$$\int_0^t e^{(t-\tau)\mathbf{E}} d\tau = \left(e^{t\mathbf{E}} - \mathbf{I}\right) \mathbf{E^{-1}} \tag{13}$$

where matrix $\mathbf{I}$ is the identity matrix, that is the $(n \times n)$ square matrix with ones on the main diagonal and zeros elsewhere, and $\mathbf{E^{-1}}$ the inverse matrix of $\mathbf{E}$.

I can immediately be deduced that the final solution in equation (12) simplifies as follows:

$$\mathbf{C_{wsm}}(t) = e^{t\mathbf{E}} \left(\mathbf{E^{-1}U}c_x + \mathbf{C_0}\right) - \mathbf{E^{-1}U}c_x \tag{14}$$

In the next sections, we employed this generic expression to go beyond and build generic physiologically-based kinetic models, that we applied to different case-study in the field of ecotoxicology.

3 Application to bioaccumulation testing

3.1 Accumulation and depuration phases

Bioaccumulation is defined as an increase in contaminant concentrations inside living organisms following uptake from the surrounding medium (living media, food, even workplace for humans). Bioaccumulation is the result of dynamical processes of uptake and elimination that can be modelled with the above ODE system (equation (2)). The extent to which bioaccumulation occurs determines the subsequent toxic effects. hence, a better knowledge on bioaccumulation enables to assess the risk related with the exposure to chemicals and to evaluate our ability to control their use and emissions in field [10].

Bioaccumulation is thus the net result of all uptake and elimination processes, such as respiratory and dietary uptake, as well as elimination by egestion, passive diffusion, metabolisation, transfer

to offspring and growth (Figure 2). Accordingly, bioaccumulation comprises both bioconcentration and biomagnification. Bioconcentration is the process of direct balance of chemicals between the exposure medium and the organism leading to increased internal concentrations. Biomagnification results in contaminant uptake from the diet leading to higher concentrations in the feeder than in the diet itself. Biomagnification leads to increased internal chemical concentration usually at higher trophic level within the food web [26, 4].

Bioaccumulation tests are usually mid-to-long term laboratory experiments designed to identify all the potential uptake pathways, including food and waterborne exposure routes [18]. Bioaccumulation tests are often called bioconcentration tests when only single route laboratory experiments are designed to obtain information concerning the ability of aquatic species to accumulate chemicals directly from water [22]. Sediment bioaccumulation tests are usually performed to determine the bioavailability of sediment contaminants and to assess their hazard through the trophic chain [21].

All bioaccumulation tests comprise an accumulation phase followed by a depuration phase [11]. During the accumulation phase, organisms are exposed to a chemical substance of interest. After a certain time period (for $t \in [0; t_c]$), with t_c fixed by the experimental design, organisms are transferred to a clean medium for the depuration phase (for $t > t_c$). The concentration of the chemical substance (and of its potential metabolites) within organisms is then measured internally at regular time points during both phases leading *in fine* to the calculation of bioaccumulation metrics [25].

If the bioaccumulation within organisms is widely studied for humans and large animals, namely, fish, birds, and farm animals [29, 15], this is not the case for smaller species, such as invertebrates [2]. However, it is equally important to decipher internal processes at the target organ level in these species, in order to better understand mechanisms implied in the subsequent effects on their fitness. Among species of interest, crustacean amphipods appears particularly promising as aquatic biomonitors of trace metals for example [2]. It is also of great importance to more deeply unravel internal routes of chemical substances between organs, after they entered within the body, a phenomenon known as organotropism [17, 27, 9].

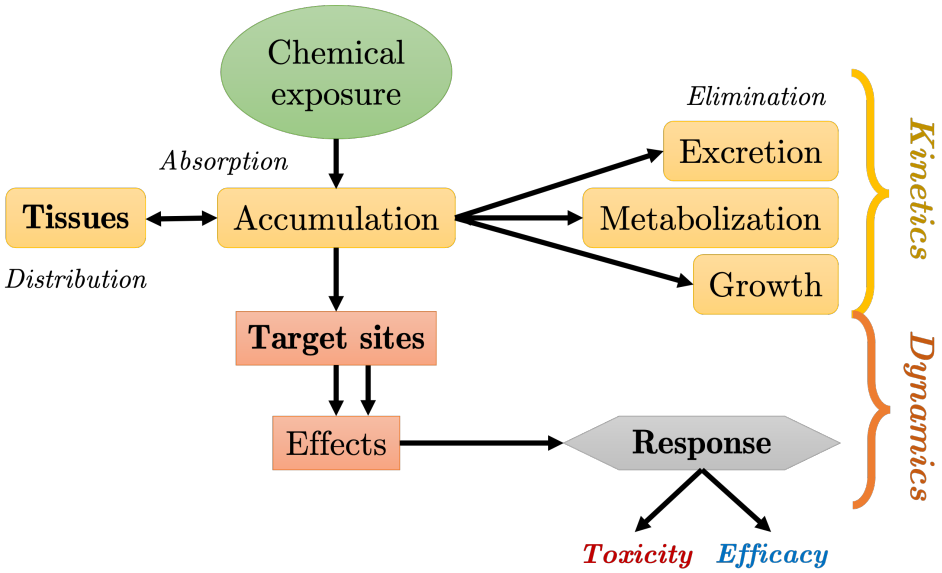

Figure 2: Absorption, Distribution, Metabolism and Excretion (ADME) processes and their relationships with effects and responses within living organisms, leading to either toxicity or efficacy depending on the type chemical substance to which they are exposed.

3.2 Generic modelling of bioaccumulation

Within this context, the generic ODE system (equation 2) may fully be applied to describe, simulate and predict what happens within and between organs of an organism when it is exposed to a given chemical substance. To this end, each organ can be associated with one model compartment, leading to the following equations for both the accumulation and the depuration phases:

Accumulation phase $(0 \leqslant t \leqslant t_c)$

$$\frac{d\mathbf{C_A}(t)}{dt} = \mathbf{U}\, c_x + \mathbf{E}\, \mathbf{C_A}(t) \tag{15}$$

Equation (15) is identical to equation (2), denoting $\mathbf{C_A}(t)$ the internal concentration at time t during the accumulation phase.

Depuration phase $(t > t_c)$

$$\frac{d\mathbf{C_D}(t)}{dt} = \mathbf{E}\, \mathbf{C_D}(t) \tag{16}$$

Variable $\mathbf{C_D}(t)$ is the internal concentration at time t during the depuration phase. Parameters and variables have the same meaning as given in Table 1.

Regarding the accumulation phase, equation (15) has a solution directly given by equation (14), the initial condition being $\mathbf{C_A}(t=0)=0$.

As a consequence, the generic solution for the **accumulation phase** writes as follows:

$$\mathbf{C_A}(t) = \left(e^{t\mathbf{E}} - \mathbf{I}\right)\mathbf{E^{-1}}\mathbf{U}c_x \tag{17}$$

Regarding the depuration phase, equation (16) is similar to equation (6), with the corresponding generic solution given by equation (7). The constant vector $\mathbf{\Omega_1}$ can be determined from the initial condition of the depuration phase that corresponds to the internal concentration reached at $t = t_c$, at the end of the accumulation phase. We must therefore solve the following equation:

$$\mathbf{C_A}(t_c) = \mathbf{C_D}(t_c) \tag{18}$$

Given solutions from equations (14) and (7), we get:

$$\mathbf{C_A}(t_c) = \left(e^{t_c\mathbf{E}} - \mathbf{I}\right)\mathbf{E^{-1}}\mathbf{U}c_x \quad \text{and} \quad \mathbf{C_D}(t_c) = e^{t_c\mathbf{E}}\mathbf{\Omega_1} \tag{19}$$

Hence, the constant vector $\mathbf{\Omega_1}$ will derived from the following equation:

$$\left(e^{t_c\mathbf{E}} - \mathbf{I}\right)\mathbf{E^{-1}}\mathbf{U}c_x = e^{t_c\mathbf{E}}\mathbf{\Omega_1} \Leftrightarrow \mathbf{\Omega_1} = \left(\mathbf{I} - e^{-t_c\mathbf{E}}\right)\mathbf{E^{-1}}\mathbf{U}c_x \tag{20}$$

The generic solution for the **depuration phase** then writes as follows:

$$\mathbf{C_D}(t) = \left(e^{t\mathbf{E}} - e^{(t-t_c)\mathbf{E^{-1}}\mathbf{U}c_x\mathbf{E}}\right)\mathbf{U}c_x \tag{21}$$

4 Case studies in ecotoxicology

This section presents three case studies with different numbers of compartments, both case studies concerning the species *Gammarus fossarum* exposed to cadmium (Cd) as studied in [13], the third one concerning the species *Danio rerio* exposed to Arsenic (As). [13] used both several one-compartment TK models compared with one four-compartment TK model, to gain knowledge on the accumulation and fate dynamic of Cd in and between gammarids' organs. Subsections 4.1 and 4.2 give the generic solutions of parameter estimates.

4.1 Case study with one compartment

Applying equation (2) with only one compartment leads to two single equations:

$$\begin{cases} \dfrac{dc_{A,i}(t)}{dt} = k_{u,1}c_x - k_{e,1}c_{A,i}(t) \quad \text{when} \quad 0 \leqslant t \leqslant t_c \quad \text{(accumulation phase)} & \text{(22a)} \\ \dfrac{dc_{D,i}(t)}{dt} = -k_{e,1}c_{D,i}(t) \quad \text{when} \quad t > t_c \quad \text{(depuration phase)} & \text{(22b)} \end{cases}$$

System of equations (22a) and (22b) can easily be solved with the method of the separation of variables (also known as the Fourier method) leading to the following system of solutions for both accumulation and depuration phases:

$$\begin{cases} c_{A,i}(t) = \dfrac{k_{u,i}}{k_{e,i}}c_x\left(1 - e^{-k_{e,i}t}\right) \quad \text{when} \quad 0 \leqslant t \leqslant t_c \quad \text{(accumulation phase)} & \text{(23a)} \\ c_{D,i}(t) = \dfrac{k_{u,i}}{k_{e,i}}c_x\left(e^{k_{e,i}(t_c - t)} - e^{-k_{e,i}t}\right) \quad \text{when} \quad t > t_c \quad \text{(depuration phase)} & \text{(23b)} \end{cases}$$

Getting the set of solutions (22) directly from the generic expressions given by the combination of both equations (17) and (21) leads exactly to the same result. Indeed, with one compartment, matrix $\mathbf{E} = -k_{e,i}$ and vector $\mathbf{U} = k_{u,i}$.

Inspired from [13], by considering only solid black arrows in Figure 3 highlights the target organs that can correspond to one compartment according to i: intestine ($i = 1$); cephalon ($i = 2$); caecum ($i = 3$); remaining tissues ($i = 4$). Each compartment has its own parameter pair for uptake ($k_{u,i}$)

Process	Organ	Parameter	Median value (in $[t]^{-1}$)
Uptake	Intestines	$k_{u,1}$	1917
	Caeca	$k_{u,2}$	1571
	Cephalons	$k_{u,3}$	91.1
	Remaining tissues	$k_{u,4}$	135
Elimination	Intestines	$k_{e,1}$	0.506
	Caeca	$k_{e,2}$	0.053
	Cephalons	$k_{e,3}$	0.060
	Remaining tissues	$k_{e,4}$	0.026

Table 2: Medians of parameters estimated from TK one-compartment models separately fitted to each organ of *Gammarus fossarum* exposed to dissolved Cd at 11.1 $\mu g.L^{-1}$ for 7 days, before being placed for 14 days under depuration conditions.

and elimination ($k_{e,i}$) rates (Table 2).

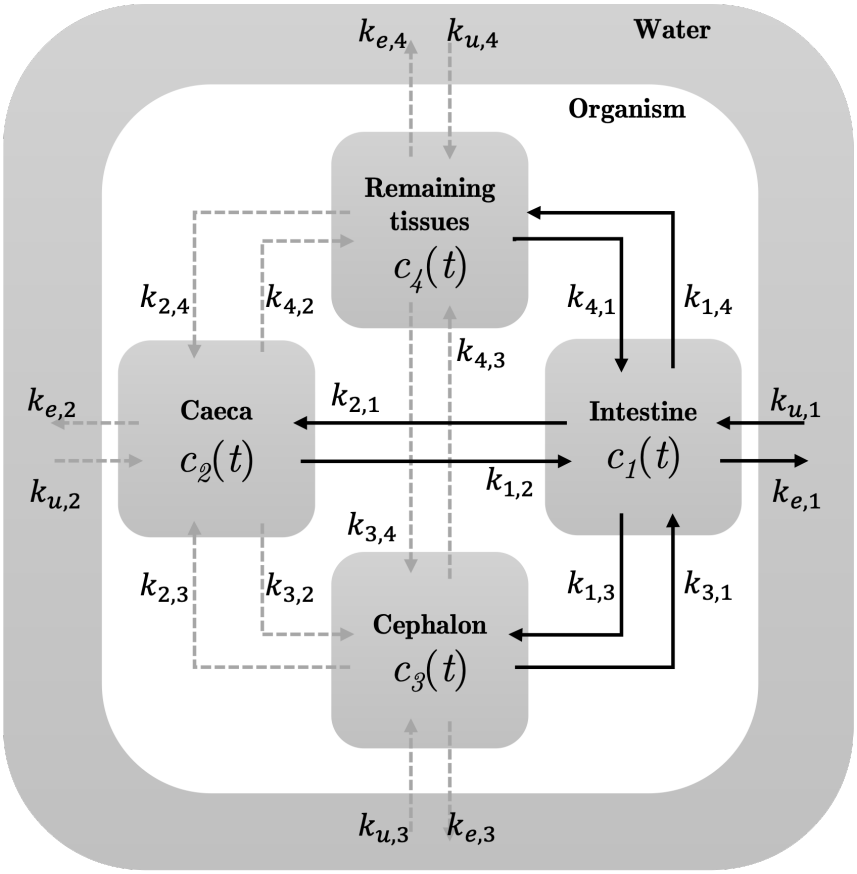

Figure 3: General schema of the multi-compartment toxicokinetic model used by [13] at the initial modelling stage when all compartments were connected to each other.

In [13], model parameters were estimated under the unified Bayesian framework proposed by [24]. In particular, parameters TK one-compartment models were fitted separately for each organ of *G. fossarum* exposed to dissolved Cd at 11.1 $\mu g.L^{-1}$ for 7 days, before being placed for 14 days under depuration conditions. Getting median parameter values as given in Table 2 allows to simulate what for example happens within intestines when is connected from all other organs (see SI for more details).

4.2 Case study with four compartments

Applying the general matrix ODE system given by the set of equations (15) and (16) to the particular case of four compartments connected by pairs (Figure 3) leads to the following writing:

$$\begin{cases} \dfrac{d\mathbf{C_A}(t)}{dt} = \mathbf{U}\, c_x + \mathbf{E}\,\mathbf{C_A}(t) \quad \text{when} \quad 0 \leqslant t \leqslant t_c \quad \text{(accumulation phase)} & \text{(24a)} \\ \dfrac{d\mathbf{C_D}(t)}{dt} = \mathbf{E}\,\mathbf{C_D}(t) \quad \text{when} \quad t > t_c \quad \text{(depuration phase)} & \text{(24b)} \end{cases}$$

with vectors and matrices defined as follows:

$$\mathbf{C_A}(t) = \mathbf{C_D}(t) = \begin{pmatrix} c_1(t) \\ c_2(t) \\ c_3(t) \\ c_4(t) \end{pmatrix} \quad \mathbf{U} = \begin{pmatrix} k_{u,1} \\ k_{u,2} \\ k_{u,3} \\ k_{u,4} \end{pmatrix} \quad \mathbf{E} = \begin{pmatrix} e_{1,1} & k_{1,2} & k_{1,3} & k_{1,4} \\ k_{2,1} & e_{2,2} & k_{2,3} & k_{2,4} \\ k_{3,1} & k_{3,2} & e_{3,3} & k_{3,4} \\ k_{4,1} & k_{4,2} & k_{4,3} & e_{4,4} \end{pmatrix} \tag{25}$$

and diagonal elements of matrix $\mathbf{E}$ defined by:

$$\begin{cases} e_{1,1} = -k_{e,1} - (k_{2,1} + k_{3,1} + k_{4,1}) & \text{(26a)} \\ e_{2,2} = -k_{e,2} - (k_{1,2} + k_{3,2} + k_{4,2}) & \text{(26b)} \\ e_{3,3} = -k_{e,3} - (k_{1,3} + k_{2,3} + k_{4,3}) & \text{(26c)} \\ e_{4,4} = -k_{e,4} - (k_{1,4} + k_{2,4} + k_{3,4}) & \text{(26d)} \end{cases}$$

The exact solution of the matrix ODE system (24) can be directly deduced from equations (17) and (21):

$$\begin{cases} \mathbf{C_A}(t) = \left(e^{t\mathbf{E}} - \mathbf{I}\right)\mathbf{E^{-1}}\mathbf{U}c_x \quad \text{when} \quad 0 \leqslant t \leqslant t_c \quad \text{(accumulation phase)} & \text{(27a)} \\ \mathbf{C_D}(t) = \left(e^{t\mathbf{E}} - e^{(t-t_c)\mathbf{E}}\right)\mathbf{E^{-1}}\mathbf{U}c_x \quad \text{when} \quad t > t_c \quad \text{(depuration phase)} & \text{(27b)} \end{cases}$$

Developing the matrix equations (27a) and (27b) finally provides both following sets of four equations for each accumulation and depuration phases:

- For the accumulation phase ($0 \leqslant t \leqslant t_c$):

$$\begin{cases} \dfrac{dc_1(t)}{dt} = k_{u,1}c_x - k_{e,1}c_1(t) + k_{1,2}c_2(t) + k_{1,3}c_3(t) + k_{1,4}c_4(t) - (k_{2,1} + k_{3,1} + k_{4,1})c_1(t) & \text{(28a)} \\ \dfrac{dc_2(t)}{dt} = k_{u,2}c_x - k_{e,2}c_2(t) + k_{2,1}c_1(t) + k_{2,3}c_3(t) + k_{2,4}c_4(t) - (k_{1,2} + k_{3,2} + k_{4,2})c_2(t) & \text{(28b)} \\ \dfrac{dc_3(t)}{dt} = k_{u,3}c_x - k_{e,3}c_3(t) + k_{3,1}c_1(t) + k_{3,2}c_2(t) + k_{3,4}c_4(t) - (k_{1,3} + k_{2,3} + k_{4,3})c_3(t) & \text{(28c)} \\ \dfrac{dc_4(t)}{dt} = k_{u,4}c_x - k_{e,4}c_4(t) + k_{4,1}c_1(t) + k_{4,2}c_2(t) + k_{4,3}c_3(t) - (k_{1,4} + k_{2,4} + k_{3,4})c_4(t) & \text{(28d)} \end{cases}$$

- For the depuration phase ($t > t_c$):

$$\begin{cases} \dfrac{dc_1(t)}{dt} = -k_{e,1}c_1(t) + k_{1,2}c_2(t) + k_{1,3}c_3(t) + k_{1,4}c_4(t) - (k_{2,1} + k_{3,1} + k_{4,1})c_1(t) & \text{(29a)} \\ \dfrac{dc_2(t)}{dt} = -k_{e,2}c_2(t) + k_{2,1}c,(t) + k_{2,3}c_3(t) + k_{2,4}c_4(t) - (k_{1,2} + k_{3,2} + k_{4,2})c_2(t) & \text{(29b)} \\ \dfrac{dc_3(t)}{dt} = -k_{e,3}c_3(t) + k_{3,1}c_1(t) + k_{3,2}c_2(t) + k_{3,4}c_4(t) - (k_{1,3} + k_{2,3} + k_{4,3})c_3(t) & \text{(29c)} \\ \dfrac{dc_4(t)}{dt} = -k_{e,4}c_4(t) + k_{4,1}c_1(t) + k_{4,2}c_2(t) + k_{4,3}c_3(t) - (k_{1,4} + k_{2,4} + k_{3,4})c_4(t) & \text{(29d)} \end{cases}$$

The four compartment model in equations (27a) and (27b), based on the matrix ODE system in equations (24a) and (24b), with its exact solution in 28 and 29, is assuming that all compartments are connected each others by pairs and with the external medium (Figure 3). This means that it is considering all incoming and outgoing arrows from all compartments. This model comprises a total of 20 parameters, plus the c_x value for the exposure concentration. Median parameter values as given in Table 3 were used to simulate what happens within each organ in terms of internal concentration dynamic, and compared to the previous results with the four independent one-compartment TK models. See SI for details.

Organ-Connection	Parameter	Median	$Q_{2.5\%}$	$Q_{97.5\%}$
Intestines (uptake)	$k_{u,1}$	3342	2720	3707
Intestines (elimination)	$k_{e,1}$	0.54	0.415	1.402
Intestines-Caeca	k_{21}	0.873	0.603	1.739
Caeca-Intestines	k_{12}	0.218	0.132	0.376
Intestines-Cephalons	k_{31}	0.059	0.034	0.124
Cephalons-Intestines	k_{13}	0.262	0.124	0.871
Intestines-Residues	k_{41}	0.069	0.049	0.126
Residues-Intestines	k_{14}	0.14	0.086	0.238
Intestines	σ_1	8.974	6.469	15.28
Caeca	σ_2	17.94	13.07	26.84
Cephalons	σ_3	1.223	0.863	1.818
Residues	σ_4	1.468	1.06	2.242

Table 3: Parameter estimates (expressed as medians and 95% uncertainty intervals) of the four-compartment model corresponding to solid black arrows in Figure 3 as provided by [13] in their Table S6. The first column stands for connected organs, either to water or to the other organs; the second column is for parameter names; the next three columns are for medians, lower and upper quantiles of parameter estimates when *G. fossarum* was exposed to Cd = 11.1 $\mu g.L^{-1}$.

As illustrated above, our generic modelling framework allows to simulate complex situations involving several compartments whatever their connections in pairs and/or with the exposure media. Let's now relate what we did in subsection 4.1 - that is simulations of four one-compartment models for each organ of *G. fossarum* exposed to Cd - with the four-compartment model developed by [13]. Indeed, [13] showed that *G. fossarum* takes up and eliminates Cd rather quickly, with the intestines and the caeca accumulating and depurating the most compared to the cephalon and the rest of the tissues. [13] also proved that a four-compartment model better describes the Cd internal contamination route than single one-compartment models for each organ. And they finally highlighted that some connections between organs and with the external medium do not exist, corresponding to the solid black arrows on Figure 3.

Such a situation in fact correspond to a nested model within the four-compartment ODE system as given by equations (24a) and (24b). This model thus comprises only 12 parameters whose values are listed in Table 3. Figure 4 below shows the simulated kinetics within the four organs. Our four curves exactly superimpose to the four median curves given in Figure 3 in [13].

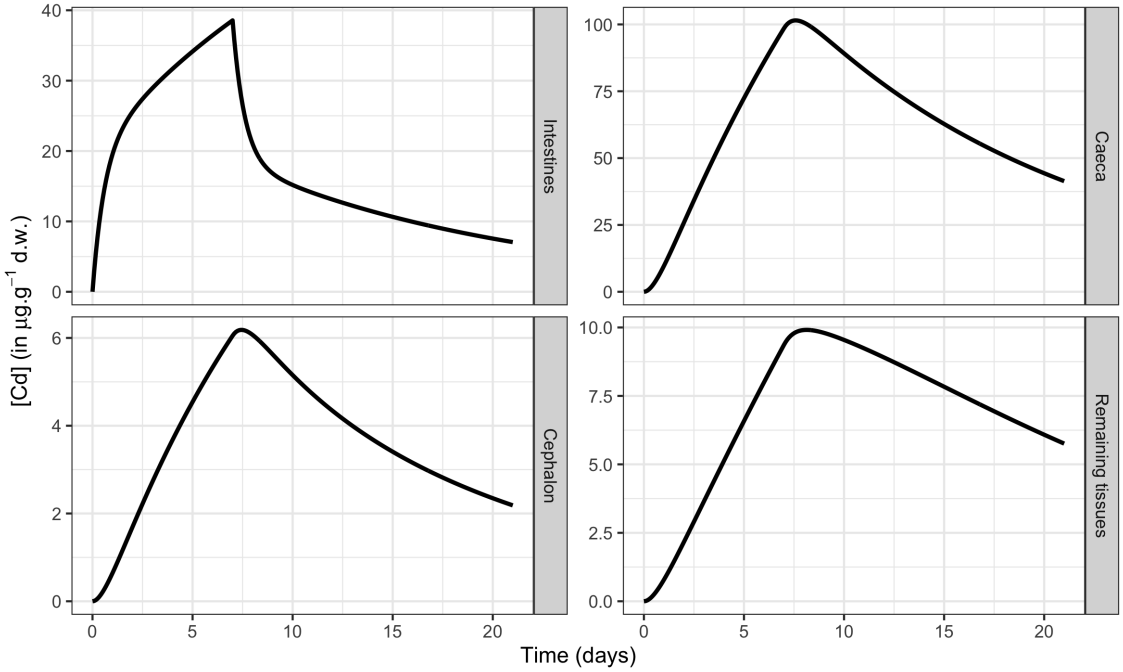

Figure 4: Simulations of internal concentration within different organs or tissues of *Gammarus fossarum* when exposed to an external concentration of cadmium equal to 11.1 $\mu g.L^{-1}$. The four-compartment PBK solution used for simulations is given in equation (27). Parameter values are given in Table 1.

4.3 Case study with six compartments

Here is a final example of the validity of our generic solution to simulate any PBK model. We reproduced what happens within zebrafish (*Danio rerio*) when exposed to Arsenic (As). [34] proposed a six-compartment model with five compartments corresponding to organs: gill ($i = 2$), intestine ($i = 3$), liver ($i = 4$), head ($i = 5$) and carcass ($i = 6$). The sixth compartment corresponds to blood ($i = 1$). The five organs were connected to blood, while gill and intestine were also connected to the external medium (As contaminated water). These assumptions are

translated in Figure 5, together with the the different parameters used for the corresponding PBK model (Table 4).

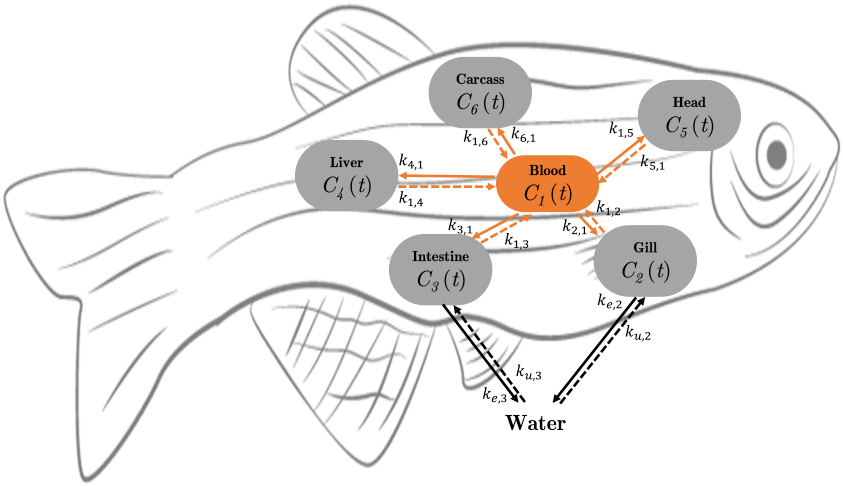

Figure 5: General scheme of the six-compartment kinetic model for zebrafish exposed to Arsenic (As, adapted from [34]). Parameters, between-organ and/or with-water connections, numerical values and units are given in Table 4.

From the generic matrix form of a PBK model we present in this paper, the model proposed by [34] writes as follows:

$$\frac{d\mathbf{C}(t)}{dt} = \mathbf{U}\, c_x + \mathbf{E}\, \mathbf{C}(t) \tag{30}$$

with vectors and matrices defined as follows:

$$\mathbf{C}(t) = \begin{pmatrix} c_1(t) & c_2(t) & c_3(t) & c_4(t) & c_5(t) & c_6(t) \end{pmatrix}^T \tag{31}$$

Where $c_i(t)$, $\forall i = 1, 6$, are the variables corresponding to internal concentrations to be simulated. Variables are $c_i(t)$ are as $\overline{w_i} C_i(t)$, $\forall i = 1, 6$, with $\overline{w_i}$ the mean wet weight of blood volume ($i = 1$) and fish organs ($\forall i = 2, 6$), while variables $C_i(t)$ are the measured concentrations of As in fish organs ($\forall i = 2, 6$, expressed in $\mu g.g^{-1}$) at time t (in days). Variable c_x is the exposure concentration of As in water (expressed in $\mu g.L^{-1}$), assumed to be constant over time.

From concentrations within organs, the concentration for the whole organism can be deduced as

follows:

$$C_{whole}(t) = \frac{1}{\sum\limits_{i=1}^{6} \overline{w_i}} \left(\sum_{i=1}^{6} \overline{w_i} c_i(t) \right) \tag{32}$$

According to our mathematical formalism, uptake parameters from water are included in the following vector:

$$\mathbf{U} = \begin{pmatrix} 0 & k_{u2} & k_{u3} & 0 & 0 & 0 \end{pmatrix}^T \tag{33}$$

while elimination parameters towards water, as well as parameters corresponding to organ-organ connections are gathered together within the following matrix:

$$\mathbf{E} = \begin{pmatrix} -\sum\limits_{j=2}^{6} k_{j,1} & k_{1,2} & k_{1,3} & k_{1,4} & k_{1,5} & k_{1,6} \\ k_{2,1} & -k_{e,2} - k_{1,2} & 0 & 0 & 0 & 0 \\ k_{3,1} & 0 & -k_{e,3} - k_{1,3} & 0 & 0 & 0 \\ k_{4,1} & 0 & 0 & -k_{1,4} & 0 & 0 \\ k_{5,1} & 0 & 0 & 0 & -k_{1,5} & 0 \\ k_{6,1} & 0 & 0 & 0 & 0 & -k_{1,6} \end{pmatrix} \tag{34}$$

The matrix ODE system (30) finally leads to the following exact solution:

$$\mathbf{C}(t) = \left(e^{t\mathbf{E}} - \mathbf{I} \right) \mathbf{E^{-1}} \mathbf{U} c_x \tag{35}$$

where c_x is the exposure concentration in water

The above matrix solution (35) can then be developed in order to retrieve the six-compartment PBPK model as constructed by [34]. Denoting the exposure concentration in water (variable c_x in our modelling) by C_{water}, we ultimately get:

$$
\begin{cases}
\overline{w_1}\dfrac{C_1(t)}{dt} = \displaystyle\sum_{j=2}^{7} k_{1,j} C_j(t)\overline{w_i} - \left(\sum_{j=2}^{7} k_{j,1}\right) C_1(t)\overline{w_1} & \text{(36a)} \\
\overline{w_2}\dfrac{C_2(t)}{dt} = k_{u,2}C_{water} + k_{2,1}C_1(t)\overline{w_1} - (k_{e,2} + k_{1,2})C_2(t)\overline{w_2} & \text{(36b)} \\
\overline{w_3}\dfrac{C_3(t)}{dt} = k_{u,3}C_{water} + k_{3,1}C_1(t)\overline{w_1} - (k_{e,3} + k_{1,3})C_3(t)\overline{w_3} & \text{(36c)} \\
\overline{w_4}\dfrac{C_4(t)}{dt} = k_{4,1}C_1(t)\overline{w_1} - k_{1,4}C_4(t)\overline{w_4} & \text{(36d)} \\
\overline{w_5}\dfrac{C_5(t)}{dt} = k_{5,1}C_1(t)\overline{w_1} - k_{1,5}C_5(t)\overline{w_5} & \text{(36e)} \\
\overline{w_6}\dfrac{C_6(t)}{dt} = k_{6,1}C_1(t)\overline{w_1} - k_{1,6}C_6(t)\overline{w_6} & \text{(36f)}
\end{cases}
$$

[34] measured internal concentrations over time in each organs and in blood during both accumulation and depuration phases. This data allowed them to estimates all their parameters. The use of a Bayesian inference framework also provided them with the quantification of the uncertainty on these parameters. [34] then deliver parameter estimates as maximum likelihood ($\mathcal{ML}$) values associated with a 95% credible interval, as partly reported in Table 4 below.

Connection	$\mathcal{ML}$	Value	Unit	Connection	$\mathcal{ML}$	Value	Unit
Water to gill	$k_{u,2}$	5.28 10^{-5}	L.d^{-1}	Gill to water	$k_{e,2}$	0.152	d^{-1}
Water to intestine	$k_{u,2}$	1.52 10^{-4}	L.d^{-1}	Intestine to water	$k_{e,2}$	0.672	d^{-1}
Blood to gill	$k_{2,1}$	76.0	d^{-1}	Gill to blood	$k_{1,2}$	58.2	d^{-1}
Blood to intestine	$k_{3,1}$	27.8	d^{-1}	Intestine to blood	$k_{1,3}$	3.94	d^{-1}
Blood to liver	$k_{4,1}$	38.5	d^{-1}	Liver to blood	$k_{1,4}$	23.6	d^{-1}
Blood to head	$k_{5,1}$	97.5	d^{-1}	head to blood	$k_{1,5}$	8.48	d^{-1}
Blood to carcass	$k_{6,1}$	7.20	d^{-1}	Carcass to blood	$k_{1,6}$	0.317	d^{-1}

Table 4: Parameter estimates for Arsenic distribution in zebrafish (from [34]). Notation $\mathcal{ML}$ stands for the estimated maximum likelihood value of the parameter.

Based on parameter $\mathcal{ML}$ values in Table 4, using fresh weight of the different organs as provided in Table S2 from [34], we performed simulations of the internal concentrations within each of the

five organs as well as in blood (variables $c_i(t)$, $\forall i = 1, 6$). As shown on Figure 6, our generic solved TK model (see equation (35)) exactly reproduce the median curves provided by [34] in their Figure 1 (solid blue lines).

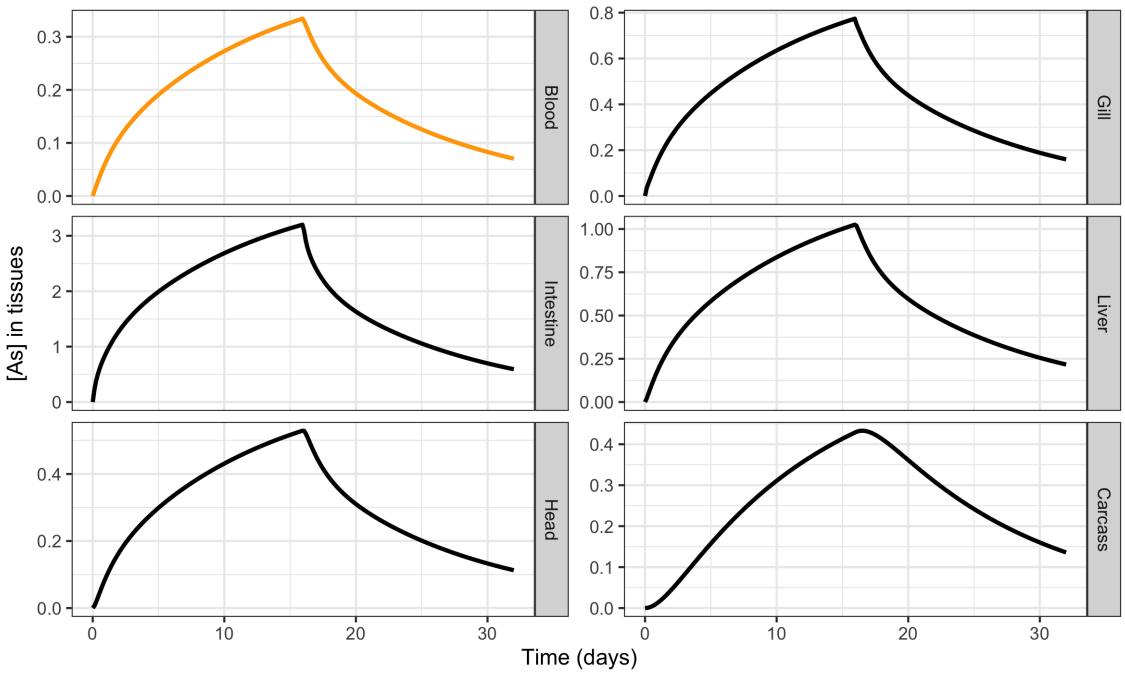

Figure 6: Simulation of the total Arsenic concentration in fish tissues and blood during the accumulation phase of 16 days (exposure concentration equal to 400 $\mu g.L^{-1}$) and the subsequent 16 days of depuration in clean medium. The PBK model used for simulations is given as a matrix solution in equation (35) with parameter values from Table 4.

5 Conclusion

Our generic solving of any full PBK model comprising as many compartments as physiologically needed, as well as all potential connections between compartments and with the external medium revealed particularly efficient in simulating diverse situations in terms of species, compounds and purpose. The four-compartment PBK model for *G. fossarum* exposed to Cd highlighted the dynamic transfer of Cd among the different organs. The six-compartment PBK model for *D. rerio*

exposed to As brought to light that intestines were the main uptake site for waterborne As, instead of gills as authors' expected.

Benefiting for this generic solution allows us to envisage the continuation of this work with confidence, in particular the implementation of a Bayesian inference framework to get parameter estimates in a quick and efficient way, based on a fully harmonized methodology. Based on preliminary results (not shown) embedded within a dedicated R-package (named `rPBTK`, and provisionally available at `https://gitlab.in2p3.fr/sandrine.charles/pbtkdb`), we already experienced that benefiting from this generic exact solution allows to divide at least by 100 the computation time of the whole process. Our previous implementation first required to numerically integrate the original ODE system, then to run the MCMC algorithm to fit the numerical solution to the accumulation-depuration data sets corresponding to the different organs and tissues. The numerical integration step was highly computationally demanding.

The next step will be to make freely and easily accessible this generic modelling framework, innovative both in the writing of the PBK model and in its exact resolution, but also in the implementation of the fitting and simulation tools. Most users, who are not necessarily modelling specialists, would be willing to use more complex PBK models, especially if necessity dictates and sufficient input data is available. Unfortunately, turnkey tools are lacking. In line with the MOSAIC platform spirit, we have therefore already undertaken the creation of a new online service that will facilitate the use of PBK models, also for beginners, with a step-by-step workflow to first upload data and select the model to fit. By default, the most complete one will be automatically proposed from which users will be able to deselect either compartments or exchanges between compartment and/or with water according to prior physiological knowledge or to try nested models and finally identify the most appropriate. Then, users will be accompanied to run the fitting process, get the results (parameter estimates and fitting plots), look at the goodness-of-fit criteria (with guidance on their interpretation), and use the model comparison criteria in case several models would have been tested. Once this calibration step achieved, users will have the possibility to run simulations, to be compared with additional data or to plan further experiments for example. in the end, all expected features of a convenient help-decision service will be offered, with a particular attention in further supporting the next generation tiered PBK modeling framework, that could become the new paradigm in human and environmental risk assessment.

This generic PBK modelling framework being firmly anchored in practice, we are now in a position to consider its coupling with mechanistic models to build a completely general modelling framework from exposure (pharmaco/toxico-kinetics) to effects (pharmaco/toxico-dynamics) on life history traits, hence defining a unifying PBKD modelling framework. We can even imagine quickly benefiting from assessment tools at populations' and communities' levels.

Acknowledgments

The authors would like to thank the BioEEnViS research federation (Biodiversity, Water, Environment, City, Health) for its financial support allowing to collaboratively achieve this study. The authors would also like to express their sincere thanks to Julie KLEINE-SCHULTJANN as part of a training course during her 5th year study at the National Institute of Applied Sciences (INSA) in Lyon (France). This work was made under the umbrella of the French GDR "Aquatic Ecotoxicology" framework, aiming at fostering stimulating scientific discussions and collaborations for more integrative approaches. The work presented in this paper was performed using the computing facilities of the CC LBBE/PRABI.

References

[1] G. J. P. Allen and D. Weihrauch. Exploring the versatility of the perfused crustacean gill as a model for transbranchial transport processes. *Comparative Biochemistry and Physiology Part - B: Biochemistry and Molecular Biology*, 254(November 2020):110572, 2021. ISSN 18791107. doi: 10.1016/j.cbpb.2021.110572.

[2] M. Amyot, B. Pinel-Alloul, P. G. Campbell, and J. C. Delsy. Total metal burdens in the freshwater amphipod *Gammarus fasciatus*: Contribution of various body parts and influence of gut contents. *Freshwater Biology*, 35(2):363–373, 1996. ISSN 00465070. doi: 10.1046/j.1365-2427.1996.00493.x.

[3] J. M. Armitage, L. Hughes, A. Sangion, and J. A. Arnot. Development and intercomparison of single and multicompartment physiologically-based toxicokinetic models: Implications for

model selection and tiered modeling frameworks. *Environment International*, 154:106557, 2021. ISSN 18736750. doi: 10.1016/j.envint.2021.106557.

[4] K. Borga. Bioaccumulation. In S. E. Jorgensen and B. D. Fath, editors, *Encyclopedia of Ecology*, pages 346–348. Academic Press, Oxford, 2008. doi: https://doi.org/10.1016/B978-008045405-4.00374-8.

[5] G. E. Box. Science and statistics. *Journal of the American Statistical Association*, 71(356): 791–799, 1976. ISSN 1537274X. doi: 10.1080/01621459.1976.10480949.

[6] M. Breen, C. L. Ring, A. Kreutz, M. R. Goldsmith, and J. F. Wambaugh. High-throughput PBTK models for in vitro to in vivo extrapolation. *Expert Opinion on Drug Metabolism and Toxicology*, 17(8):903–921, 2021. ISSN 17447607. doi: 10.1080/17425255.2021.1935867.

[7] M. Brinkmann, K. Eichbaum, U. Kammann, S. Hudjetz, C. Cofalla, S. Buchinger, G. Reifferscheid, H. Schüttrumpf, T. Preuss, and H. Hollert. Physiologically-based toxicokinetic models help identifying the key factors affecting contaminant uptake during flood events. *Aquatic Toxicology*, 152:38–46, 2014. ISSN 18791514. doi: 10.1016/j.aquatox.2014.03.021.

[8] S. Charles, A. Ratier, and C. Lopes. Generic solving of one-compartment toxicokinetic models. *Journal of Exploratory Research in Pharmacology*, submitted, 2021. doi: 10.1101/2021.05.06.442956v1.

[9] W. Chen, A. D. Hoffmann, H. Liu, and X. Liu. Organotropism: new insights into molecular mechanisms of breast cancer metastasis. *Precision Oncology*, 2(1), 2018. doi: 10.1038/s41698-018-0047-0.

[10] K. Chojnacka and M. Mikulewicz. Bioaccumulation. In P. Wexler, editor, *Encyclopedia of Toxicology (Third Edition)*, pages 456–460. Academic Press, Oxford, third edition edition, 2014. doi: https://doi.org/10.1016/B978-0-12-386454-3.01039-3.

[11] European Commission. European Commission (EU) No 283/2013 of 1 March 2013 setting out the data requirements for active substances, in accordance with Regulation (EC) No 1107/2009 of the European Parliament and of the Council concerning the placing of plant protection produc, 2013.

[12] M. N. Fransson, L. Barregard, G. Sallsten, M. Akerstrom, and G. Johanson. Physiologically-based toxicokinetic model for cadmium using markov-chain monte carlo analysis of concentrations in blood, urine, and kidney cortex from living kidney donors. *Toxicological Sciences*, 141(2):365–376, 2014. ISSN 10960929. doi: 10.1093/toxsci/kfu129.

[13] O. Gestin, T. Lacoue-labarthe, M. Coquery, N. Delorme, L. Garnero, L. Dherret, O. Geffard, and C. Lopes. One and multi-compartments toxico-kinetic modeling to understand metals ' organotropism and fate in *Gammarus fossarum*. *Environment international*, 156(April):1–9, 2021. doi: 10.1016/j.envint.2021.106625.

[14] A. Grech, C. Brochot, J.-L. Dorne, N. Quignot, F. Y. Bois, and R. Beaudouin. Toxicokinetic models and related tools in environmental risk assessment of chemicals. *Science of the Total Environment*, 578:1–15, 2017.

[15] A. Grech, C. Tebby, C. Brochot, F. Y. Bois, A. Bado-Nilles, J. L. Dorne, N. Quignot, and R. Beaudouin. Generic physiologically-based toxicokinetic modelling for fish: Integration of environmental factors and species variability. *Science of the Total Environment*, 651:516–531, 2019. doi: 10.1016/j.scitotenv.2018.09.163.

[16] J. W. Green, T. Springer, and H. Holbech. *Statistical Analysis of Ecotoxicity Studies*. John Wiley & Sons, wiley edition, jul 2018. ISBN 9781119488828. URL `www.wiley.com/go/Green/StatAnalysEcotoxicStudy`.

[17] Y.-R. Ju, W.-Y. Chen, S. Singh, and C.-M. Liao. Trade-offs between elimination and detoxification in rainbow trout and common bivalve molluscs exposed to metal stressors. *Chemosphere*, 85(6):1048–1056, 2011. doi: https://doi.org/10.1016/j.chemosphere.2011.07.033.

[18] I. Marigomez. Environmental risk assessment, marine. In P. Wexler, editor, *Encyclopedia of Toxicology (Third Edition)*, pages 398–401. Academic Press, Oxford, third edition edition, 2014. doi: https://doi.org/10.1016/B978-0-12-386454-3.00556-X.

[19] C. Mit, A. Bado-Nilles, G. Daniele, B. Giroud, E. Vulliet, and R. Beaudouin. The toxicokinetics of bisphenol A and its metabolites in fish elucidated by a PBTK model. *Aquatic Toxicology*, 247(April):106174, 2022. ISSN 0166445X. doi: 10.1016/j.aquatox.2022.106174.

[20] OECD. Guidance document on the characterisation , validation and reporting of Physiologically Based Kinetic (PBK) models for regulatory purposes. *Series on Testing and Assessment*, No. 331, 2021. URL `http://www.oecd.org/chemicalsafety/risk-assessment/guidance-document-on-the-characterisation-validation-and-reporting-of-physiologically-b` `pdf`.

[21] Organisation for Economic Co-operation and Development. *Test No 315: Bioaccumulation in sediment-dwelling benthic oligochaetes*, volume 315. OECD Publishing, 2008. doi: 10.1787/2074577x.

[22] Organisation for Economic Co-operation and Development. *Test No. 305: Bioaccumulation in Fish: Aqueous and Dietary Exposure*, volume 305. OECD Publishing, 2012. doi: 10.1787/9789264185296-en.

[23] A. Paini, J. A. Leonard, E. Joossens, J. G. Bessems, A. Desalegn, J. L. Dorne, J. P. Gosling, M. B. Heringa, M. Klaric, T. Kliment, N. I. Kramer, G. Loizou, J. Louisse, A. Lumen, J. C. Madden, E. A. Patterson, S. Proença, A. Punt, R. W. Setzer, N. Suciu, J. Troutman, M. Yoon, A. Worth, and Y. M. Tan. Next generation physiologically based kinetic (NG-PBK) models in support of regulatory decision making. *Computational Toxicology*, 9(November 2018):61–72, 2019. ISSN 24681113. doi: 10.1016/j.comtox.2018.11.002.

[24] A. Ratier, C. Lopes, P. Labadie, N. Budzinski, Hélène Delorme, H. Quéau, L. Peluhet, O. Geffard, and M. Babut. A unified Bayesian framework for estimating model parameters for the bioaccumulation of organic chemicals by benthic invertebrates: proof of concept with PCB153 and two freshwater species. *Ecotoxicology and Environmental Safety*, 180:33–42, 2019.

[25] A. Ratier, C. Lopes, G. Multari, V. Mazerolles, P. Carpentier, and S. Charles. New perspectives on the calculation of bioaccumulation metrics for active substances in living organisms. *Integrated Environmental Assessment and Management*, 18(1):10–18, 2021. doi: 10.1101/2020.07.07.185835.

[26] H. T. Ratte. Bioaccumulation and toxicity of silver compounds: A review. *Environmental Toxicology and Chemistry*, 18(1):89–108, 1999. doi: 10.1002/etc.5620180112.

[27] T. L. Rocha, T. Gomes, J. P. Pinheiro, V. S. Sousa, L. M. Nunes, M. R. Teixeira, and M. J. Bebianno. Toxicokinetics and tissue distribution of cadmium-based quantum dots in the marine mussel *Mytilus galloprovincialis*. *Environmental Pollution*, 204:207–214, 2015. ISSN 0269-7491. doi: https://doi.org/10.1016/j.envpol.2015.05.008.

[28] L. M. Sweeney, L. MacCalman, L. T. Haber, E. D. Kuempel, and C. L. Tran. Bayesian evaluation of a physiologically-based pharmacokinetic (PBPK) model of long-term kinetics of metal nanoparticles in rats. *Regulatory Toxicology and Pharmacology*, 73(1):151–163, 2015. ISSN 10960295. doi: 10.1016/j.yrtph.2015.06.019.

[29] J. V. Tarazona, C. Rodriguez, E. Alonso, M. Saez, F. Gonzalez, M. D. San Andres, B. Jimenez, and M. I. San Andres. Toxicokinetics of perfluorooctane sulfonate in birds under environmentally realistic exposure conditions and development of a kinetic predictive model. *Toxicology Letters*, 232(2):363–368, jan 2015. doi: 10.1016/j.toxlet.2014.11.022.

[30] E. Testai, C. Bechaux, F. M. Buratti, K. Darney, E. D. Consiglio, E. E. J. Kasteel, N. I. Kramer, L. S. Lautz, N. Santori, Z.-v. Skaperd, D. Kouretas, L. Turco, and S. Vichi. Modelling human variability in toxicokinetic and toxicodynamic processes using Bayesian meta-analysis , physiologically-based modelling and in vitro systems. *EFSA Supporting publication*, EN-6504 (February), 2021. doi: 10.2903/sp.efsa.2021.EN-6504.

[31] C. V. Thompson, J. W. Firman, M. R. Goldsmith, C. M. Grulke, Y. M. Tan, A. Paini, P. E. Penson, R. R. Sayre, S. Webb, and J. C. Madden. A Systematic Review of Published Physiologically-based Kinetic Models and an Assessment of their Chemical Space Coverage. *Alternatives to laboratory animals : ATLA*, 49(5):197–208, 2021. ISSN 02611929. doi: 10.1177/02611929211060264.

[32] M. G. Vijver, C. A. Van Gestel, R. P. Lanno, N. M. Van Straalen, and W. J. Peijnenburg. Internal metal sequestration and its ecotoxicological relevance: A review. *Environmental Science and Technology*, 38(18):4705–4712, 2004. ISSN 0013936X. doi: 10.1021/es040354g.

[33] W. X. Wang and P. S. Rainbow. Comparative approaches to understand metal bioaccumulation in aquatic animals. *Comparative Biochemistry and Physiology - C Toxicology and Pharmacology*, 148(4):315–323, 2008. ISSN 15320456. doi: 10.1016/j.cbpc.2008.04.003.

[34] J. Zhang, Q.-G. Tan, L. Huang, Z. Ye, X. Wang, T. Xiao, Y. Wu, W. Zhang, and B. Yan. Intestinal uptake and low transformation increase the bioaccumulation of inorganic arsenic in freshwater zebrafish. *Journal of Hazardous Materials*, 434(April):128904, 2022. ISSN 03043894. doi: 10.1016/j.jhazmat.2022.128904.

[35] L. Zhang, V. Sinha, S. T. Forgue, S. Callies, L. Ni, R. Peck, and S. R. Allerheiligen. Model-based drug development: The road to quantitative pharmacology. *Journal of Pharmacokinetics and Pharmacodynamics*, 33(3):369–393, 2006. ISSN 1567567X. doi: 10.1007/s10928-006-9010-8.

[36] Y. Zhang, J. Feng, Y. Gao, X. Liu, L. Qu, and L. Zhu. Physiologically based toxicokinetic and toxicodynamic (PBTK-TD) modelling of Cd and Pb exposure in adult zebrafish Danio rerio: Accumulation and toxicity. *Environmental Pollution*, 249:959–968, 2019. ISSN 18736424. doi: 10.1016/j.envpol.2019.03.115.